

BBN ACOUSTIC TECHNOLOGIES

A Division of BBN Corporation

BBN Report No.: 8139

MISSISSIPPI CANYON SOUND PROPAGATION STUDY

February 1996

Kevin LePage
Charles Malme
Rafal Mlawski
Peter Krumhansl

Prepared by:

BBN Acoustic Technologies
A Division of BBN Corporation
70 Fawcett Street
Cambridge, MA 02138

Prepared for:

Exxon Exploration Company
222 Benmar
Houston, TX 77060



BBN Report No.: 8139

MISSISSIPPI CANYON SOUND PROPAGATION STUDY

February 1996

Kevin LePage
Charles Malme
Rafal Mlawski
Peter Krumhansl

Prepared by:

BBN Acoustic Technologies
A Division of BBN Corporation
70 Fawcett Street
Cambridge, MA 02138

Prepared for:

Exxon Exploration Company
222 Benmar
Houston, Texas 77002

Table of Contents

ABSTRACT.....	1
1. Description of Experiments	2
1.1 Source ship.....	2
1.2 Receiver ship and receiving array.....	3
1.4 Post-processing system.....	6
1.5 Navigation.....	6
1.6 Weather.....	6
1.7 Sound speed.....	6
2. Data Processing.....	7
3. Results.....	15
3.1 Source Level Estimation—Experiment 1	15
3.2 Broadside to endfire ratio	17
3.3 Determination of X log R propagation law and isopleths	20
3.3.1 190 dB re μ Pa isopleth.....	21
3.3.2 Determination of the 180 dB re μ Pa isopleths.....	21
3.3.3 Determination of 160 dB re μ Pa isopleth for Experiments 2, 3 and 4.....	23
4. Conclusions.....	27

List of Tables

Table 1. Vertical array specifications	4
Table 2. Array to DAT channel mapping for Experiment 1	5
Table 3. Array to DAT channel mappings for Experiments 2, 3 and 4	5
Table 4. Ranges to the 190, 180 and 160 dB re μ Pa average pulse pressure isopleths for the Mississippi Canyon experiment. The three ranges given for the 160 dB re μ Pa isopleth are for three different propagation scenarios of down, cross and up-slope.....	27

List of Figures

Figure 1. Historical sound speed profile for the Mississippi Canyon region of the Gulf of Mexico.....	8
Figure 2. Experiment 1—Close approach test geometry	9
Figure 3. Experiment 2—Down-slope test geometry.	10
Figure 4. Experiment 3—Cross-slope test geometry.....	11
Figure 5. Experiment 4—Up-slope test geometry.	12
Figure 6. Low and highpass analog filters (green) and the corrective effect of the digital compensating filter (red)	14
Figure 7. Peak amplitudes measured during the close pass experiment as a function of range.....	16
Figure 8. Peak source levels estimated from close pass peak amplitudes, as a function of range.....	18
Figure 9. Peak source levels as a function of array to receiver bearing.....	19

Figure 10. Experiment 1—Average pulse pressure level as a function of range
(endfire corrected +8.5 dB).....22

Figure 11. Experiment 2—Average pulse pressure level as a function of range
(endfire corrected +8.5 dB).....24

Figure 12. Experiment 3—Average pulse pressure level as a function of range
(endfire corrected +8.5 dB).....25

Figure 13. Experiment 4—Average pulse pressure level as a function of range
(endfire corrected +8.5 dB).....26

ABSTRACT

During the period between October 21st and 22nd, 1995, BBN conducted a test in the Mississippi Canyon region of the Gulf of Mexico to determine the characteristics of acoustic propagation in the vicinity of a 3-D seismic source array. The purpose of the experiment was to:

- 1) Determine the ranges to the 190, 180 and 160 dB re 1 μ Pa average pulse pressure isopleths (as defined by Malme et. al in earlier marine mammal sound exposure studies) at beam aspect to the source array.
- 2) Determine the beam aspect to end-fire peak sound pressure level ratio in the horizontal plane for the array in the near and far field.
- 3) Verify the peak source level of the array at broadside aspect in the horizontal plane.
- 4) Determine a best fit $X \log R$ (where R is the range) propagation model parameterization which could be used to predict average pulse pressure as a function of range in a similar environment for different types of source arrays.

1. Description of Experiments

A total of four experiments were conducted between approximately 21:00 (UTC) October 22nd and 10:00 October 23rd. The experiments were all conducted at approximately 28 31 N Lat and 89 34 W Long in the vicinity of the northeastern approaches of the Mississippi canyon near Sackett shoal. The water depth during the experiments varied between 100 and 500 meters. The experiments are summarized below:

Experiment 1, which is noted as Run 3 in the experiment log book, consisted of a series of 4 close passes of the source ship to the receiving array, to determine the source level and the directivity of the source array.

Experiment 2 (Run 4) was a long range propagation experiment in a down-slope geometry. The receiving array was held stationary as the source array was towed northeast into shallower waters, out to a range of 10 km. In order to determine the far-field directivity of the source array, as filtered through the propagation environment, two figure-eight maneuvers were executed by the source ship at the 5 and 10 km marks.

Experiment 3 (Run 5), was a cross-slope long range propagation experiment where the source was towed east away from the receiving array roughly parallel to contours of constant water depth to a range of 10 km. During this experiment no figure-eights were executed.

Experiment 4 (Run 6) was an up-slope long range propagation experiment, where the receiving array was deployed in close vicinity to Sackett shoal and the source array was towed southwest into deeper waters. As in Experiment 2, two figure-eight maneuvers were again executed at 5 and 10 km in order to estimate the end-fire to broadside directivity ratio of the airgun array as filtered through the propagation environment.

1.1 Source ship

The source ship was the RV Sea Star, a Chouest boat operated by Geco-Prakla which deployed an eighteen element seismic airgun array. The array was deployed at a depth of 6 m, and had a physical aperture of 18x18 m, defined by three strings of airguns of 18 m in length containing 6 guns each deployed 9 m apart. The forward starboard gun of this array was held in reserve in the event of a failure of another gun. The instantaneous peak

level source strength of the airgun array reduced to a reference distance of 1 m was estimated by Exxon before the experiment to be 23.7 Bar-m at broadside for a zero depression/elevation angle (0 deg D/E), and 106 Bar-m in the main lobe directed towards the bottom (90 deg D/E) for seismic profiling. In engineering units familiar to underwater acousticians, these source levels correspond to 247.5 dB re $\mu\text{Pa-m}$ at 0 deg D/E at broadside, and 260.5 dB re 1 $\mu\text{Pa-m}$ at 90 deg D/E. The source array firing sequence for these experiments was designed both to measure the output of the full array and to measure propagation with a single airgun. A single airgun shot was followed by a shot of the full source array, followed by a single string shot and then another full array shot. This sequence took 30 seconds, with ten seconds between shots, and was repeated every 40 seconds. Thus there were 10 seconds between all shots, regardless of type.

1.2 Receiver ship and receiving array

The receiving vessel was the RV Sea Storm, a supply vessel also operated by Geco-Prakla. The receiving array was deployed off a steel raft which floated approximately 30 m from the stern of the ship. The receiving array had a vertical aperture of 90 m, with hydrophone elements deployed every 10 m. The array was decoupled from the raft using shock cord, and was weighted using chain wrapped in Arno tape. The portion of the array leading from the raft to the side rail of the Sea Storm was strain relieved with a 1 in nylon hawser, and was floated using 3 Norwegian buoys.

The hydrophones were manufactured by High Tech, Inc. and consisted of 8 HTI-194 and 1 HTI-215. These are cylindrical piezo-electric phones with built-in current-mode preamplifiers for 2 wire low noise operation. The array was a hair-faired kevlar cable deployed with the assistance of a reel roller.

The hydrophones deployed on the array cable had the depths, sensitivities and channel numbers outlined in Table 1.

The 3.2 kHz rolloff of was unintentionally caused by a manufacturing defect and was compensated during the post processing of the data. Exxon specifically asked for 20 kHz rolloff hydrophones.

The dry end of the hydrophone cable was lead to a preamplifier with 20 dB of gain per channel. From the preamplifier the signals were passed through a bank of Ithaco

Table 1. Vertical array specifications

Channel #	Depth (m)	Sensitivity dB re $\mu\text{Pa/V}$	Rolloff (kHz)	Serial #
8	10	194.59	3.2	101001
7	20	194.71	3.2	101005
6	30	194.67	3.2	101002
5	40	194.8	3.2	101006
4	50	194.68	3.2	101007
3	60	194.88	3.2	101008
2	70	194.67	3.2	101004
1	80	213.8	20	2006
0	98	194.68	3.2	101003

amplifiers with 10 Hz high-pass filters. This filtering operation was carried out to reduce saturation of the recording instruments with low frequency hydrodynamic noise. The recording instruments themselves were Teac models T135 and T145 which functioned identically for the purposes of this study. These DAT recorders have 80 kHz total bandwidth and 14 bit A/D converters. The bandwidth on each recorder was divided among 4 channels recording from 0-20kHz.

The two recorders provided a total of 8 channels of recording capability, but since there were 9 hydrophones, it was necessary to exclude one of the hydrophone channels during the experiments. It was desired to record a representative sampling of the aperture of the array on the T135 for the ease of processing. For Experiments 2,3 and 4, hydrophone channels 0,3,6 and 8 were recorded on the four channels of this instrument. However, since the most important channel for the near-field experiments was the desensitized hydrophone on channel 1, because it enabled the source signature to be recorded at very close range without clipping, the channel was recorded in lieu of channel 3 during Experiment 1. The DAT channel to vertical array channel mappings for the two different setups are recorded in Tables 2 and 3.

The Ithaco amplifiers were capable of passing approximately 7 Volts full scale. The hydrophones themselves were capable of generating up to 1 Volt full scale. The preamps

passed up to 10 volts full scale. With this system, the normal sensitivity phones could linearly record levels up to 191.5 dB re μ Pa. The desensitized phone could record levels

Table 2. Array to DAT channel mapping for Experiment 1

Channel #	T135 Channel #	T145 Channel #
8	4	
7		4
6	3	
5		3
4		2
3		
2		1
1	2	
0	1	

Table 3. Array to DAT channel mappings for Experiments 2,3 and 4

Channel #	T135 Channel #	T145 Channel #
8	4	
7		4
6	3	
5		3
4		2
3	2	
2		1
1		
0	1	

up to 211 dB re μ Pa when the sensitivity of the Teac's was set at 20 Volts. In practice clipping was only experienced on the normal sensitivity (~194 dB) channels when the source passed to within 160 m of the vertical array during Experiment 1. At all times the desensitized phone at 80 m was recorded without clipping.

Real time monitoring of the data was carried out with a HP 3561 digital spectrum analyzer with a high frequency compensating filter. The network of the compensating filter was designed to remove the effects of the 6 dB per octave 3.2 kHz low pass filters installed in the hydrophone elements themselves. The analyzer was used in the trigger mode to capture the peak amplitudes of signals coming out of this compensating filter, so that it was possible to log the peak levels in Volts in real time.

1.4 Post-processing system

The post processing was performed with a 100 MHz Pentium based PC with 44 Mbytes of RAM and 2 Gbytes of hard disk space. The data was played back with a Teac DAT interface card driven by QuickVu software. All post analysis was performed in the MATLAB environment. Scripts were written which read the binary files produced by QuickVu and corrected for recording gains and scaled volts to μPa . All subsequent processing was performed in the engineering units of μPa .

1.5 Navigation

Navigation information for the M/V Sea Star was provided after the sea test by Mr. Thor Bakke of Geco Prakla. The position of the Sea Star was determined by differential GPS and the relative position of the source array was determined by a laser range-finder. An eight column ACSII file contained the line, shot, latitude, longitude, easting, northing, universal time constant (UTC), ship heading, and shot schedule (binary string). The M/V Sea Storm tail buoy navigation information was provided by Mr. Sean Chard of John Chance and Assoc. This information was transmitted to BBN in four column ACSII file format with fields of date, local time, easting and northing. M/V Sea Star time was UTC. The Sea Storm time was local time. When the M/V Sea Storm time was corrected to UTC, it was 11 seconds ahead of M/V Sea Star time. The bearing from the M/V Sea Star to the M/V Sea Storm and thence the array angle to the receiver were obtained by post processing.

1.6 Weather

Weather was variable, with Sea State 1 and light SE breezes at the beginning of the experiment building to a 12-16 Kt SE wind and Sea State 3 at the end of the experiment. The moderate seas at the end of the experiment caused significant noise on the hydrophones in the middle of the vertical array. It is speculated that most of this noise was strum although significant vertical forces were also applied to the array by the surging tail buoy, and the problem may have been mechanical.

1.7 Sound speed

A single XBT cast by the personnel on the M/V Sea Star yielded the sound velocities over the upper 20 m of the water column. Historical profiles for the region are

significantly downward refracting, as illustrated in Figure 1. The measured sound speeds are shown superimposed on the historical data. The slightly upward refracting mixed layer measured during the experiment is consistent with the fact that a significant storm swept the area in the previous 48 hours. The implication of the downward refracting profile below 40 m is that the losses measured during this experiment may differ significantly from those measured in a mixed layer environment. Since a downward refracting profile causes acoustic energy to interact more often with the bottom, it is likely that these measurements represent a lower bound on peak received level at a given range.

2. Data Processing

Of the four experiments conducted, BBN performed data reduction on the third close pass measured during Experiment 1, the 10 km long northeast up-slope transit of Experiment 2, the 11 km cross-slope transit of Experiment 3, and on the 10 km long southwest down-slope transit of Experiment 4. Note that the down-slope transit of the source vessel away from the receiver represents an up-slope propagation scenario and visa-versa. The navigation data from these five data sets are illustrated in Figures 2, 3, 4, and 5.

In these figures, the position of the source is illustrated in green, and the position of the receiving array is illustrated in red. In addition, vectors have been drawn from each source position. These vectors are intended to illustrate how the relative angle from the source array to the receiving array changes as a function of position. This angle is important, for it is known that the airgun array radiates higher peak levels in the broadside direction than in the end-fire direction. In these figures, the azimuth of the array is indicated by green arrows which indicate the relative bearing, e.g. right (90 deg relative bearing), left (270 deg), straight up (0 deg), and down (180 deg). It may be noticed that for all the experiments, the array is nearly always in an end-fire aspect from the point of view of the vertical array. This causes the levels measured to be lower than they would be for the same range, if the array were in a broadside aspect.

Using the QuickVu software to operate the DAT recorders, four of the eight recorded hydrophones from the vertical line array were scanned for events corresponding to the firing of the source array. Full airgun array events were easily identified using the QuickVu software and saved in Volts in binary QuickVu files. A MATLAB script was

XBT sound speed measurements superimposed on GDEM database sound speeds for Gulf of Mexico

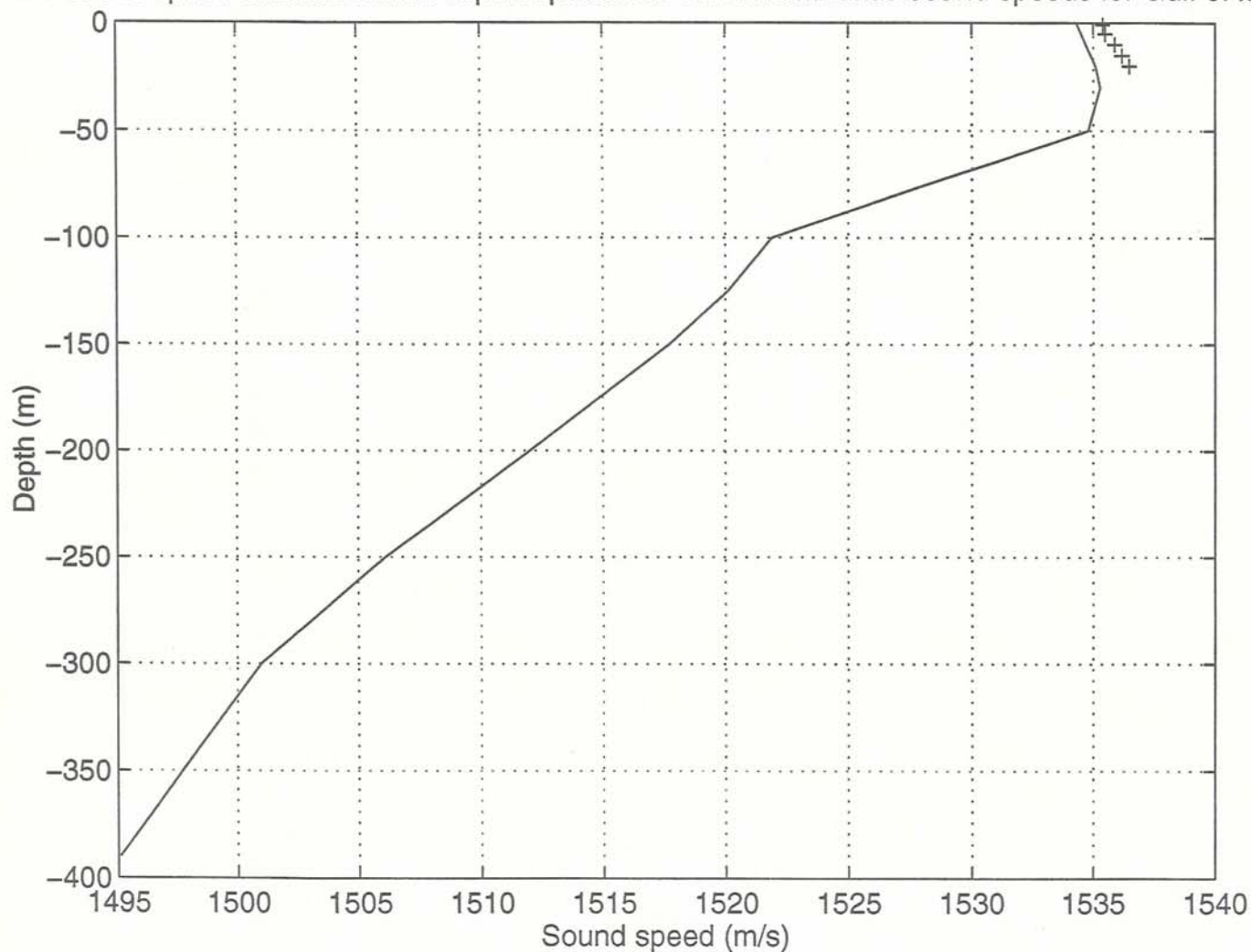


Figure 1. Historical sound speed profile for the Mississippi Canyon region of the Gulf of Mexico. Data obtained by in situ XBT measurements are shown superimposed on the figure with X's.

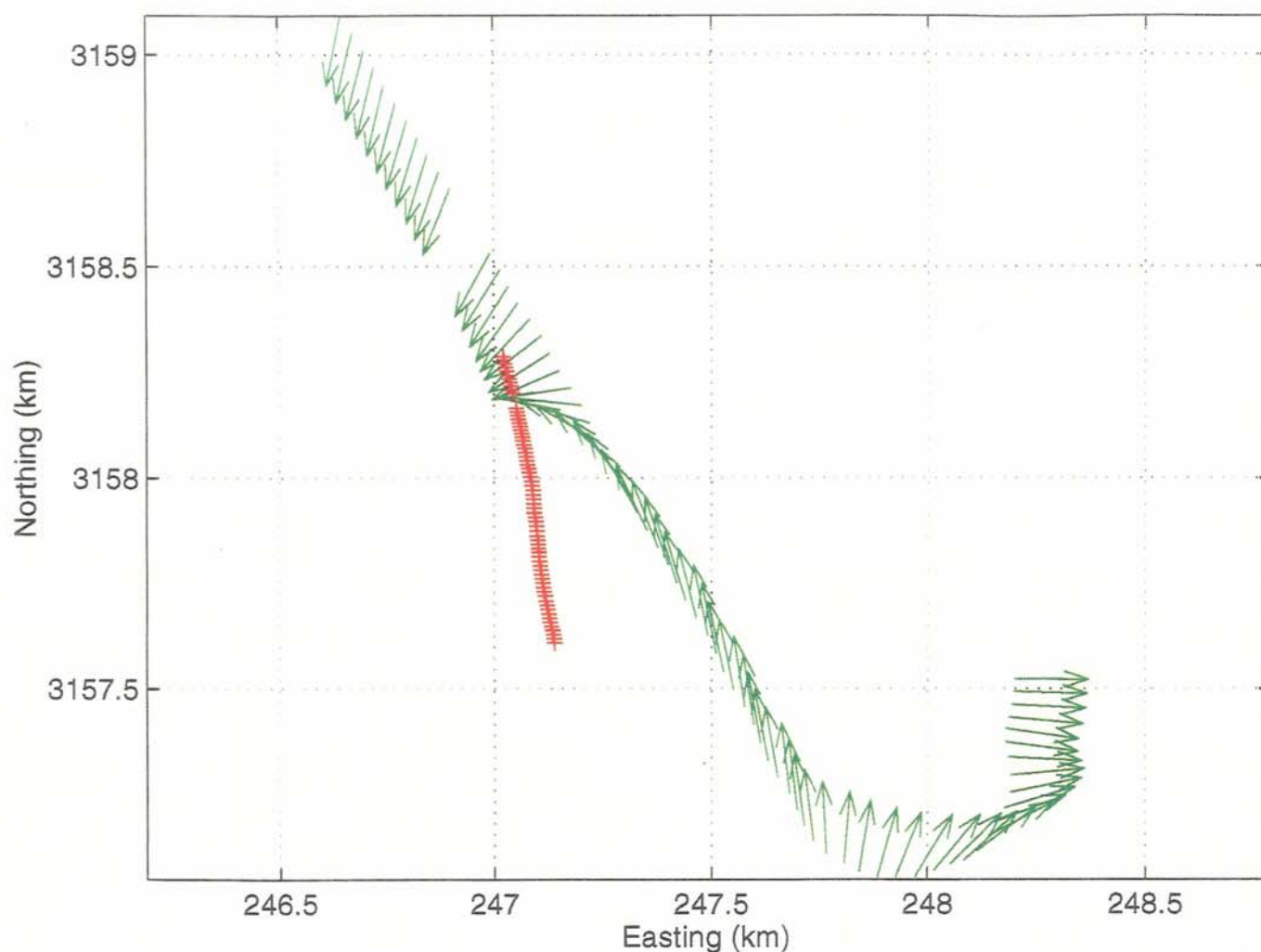


Figure 2. Experiment 1—Close approach test geometry. The red crosses indicate the position of the receiving vessel M/V Sea Storm. The position of the source vessel M/V Sea Star is indicated by the origins of the green arrows. The direction of the green arrows indicates the array angle from the source to the receiver. Green arrows which point to the right indicate that the receiver was at Starboard broadside aspect to the source array. Green arrows which point down indicate the receiver was stern aspect to the source array. Green arrows which point to the left indicate that the receiver was at Port broadside aspect to the array. Green arrows which point up indicate that the receiver was forward of the array.

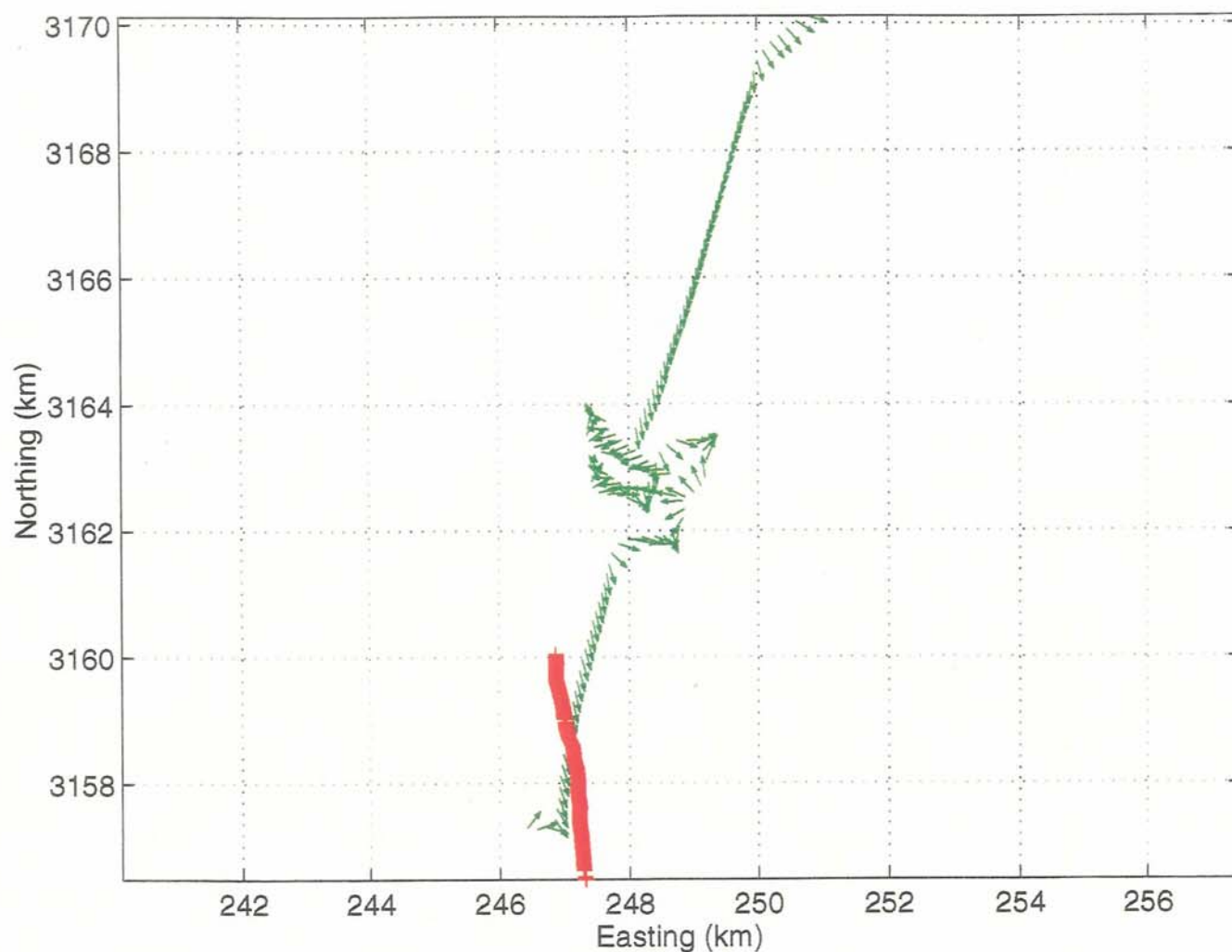


Figure 3. Experiment 2—Down-slope test geometry. The red crosses indicate the position of the receiving vessel M/V Sea Storm. The position of the source vessel M/V Sea Star is indicated by the origins of the green arrows. See Figure 2 for an explanation of the orientation of the green arrows.

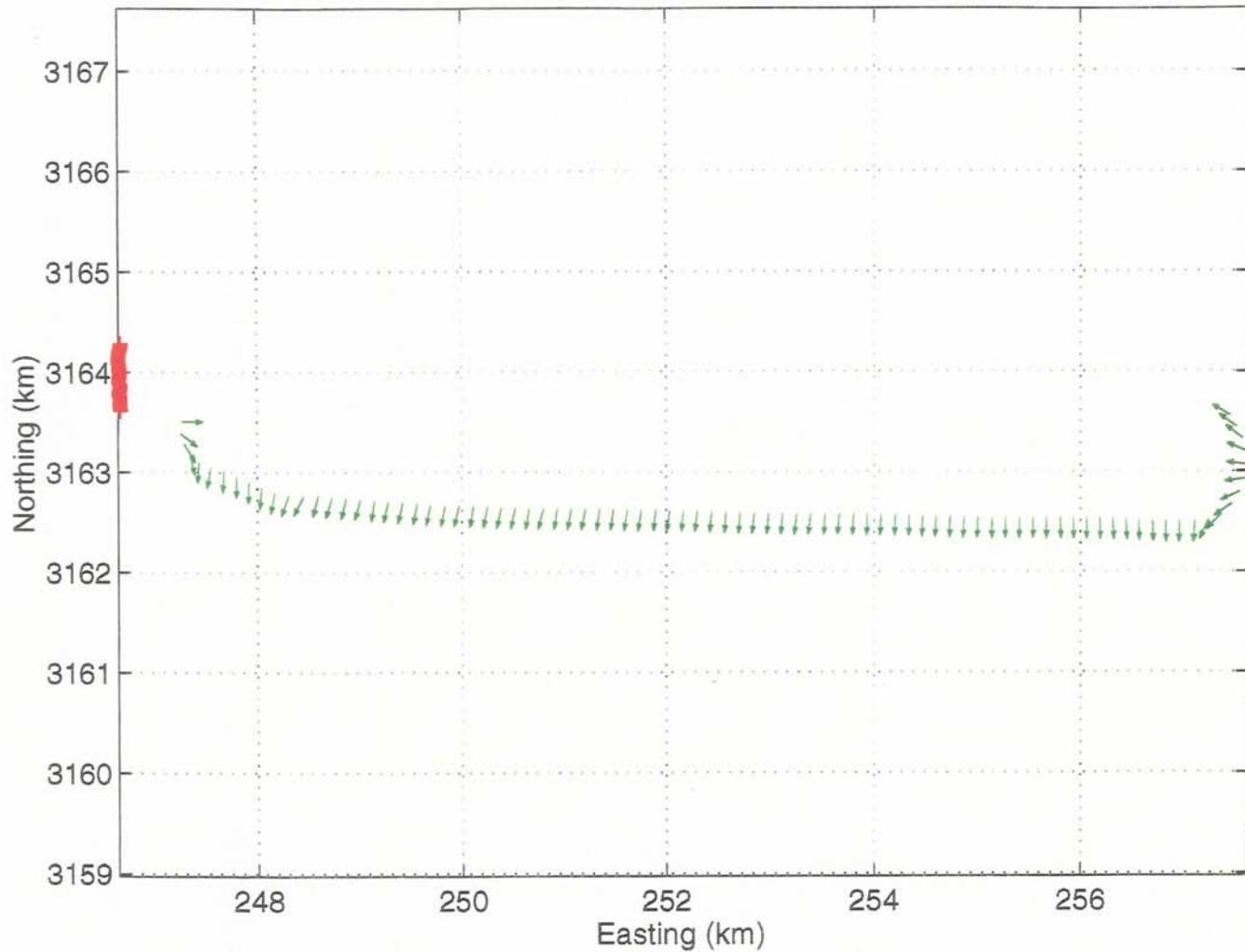


Figure 4. Experiment 3—Cross-slope test geometry. The red crosses indicate the position of the receiving vessel M/V Sea Storm. The position of the source vessel M/V Sea Star is indicated by the origins of the green arrows. See Figure 2 for an explanation of the orientation of the green arrows.

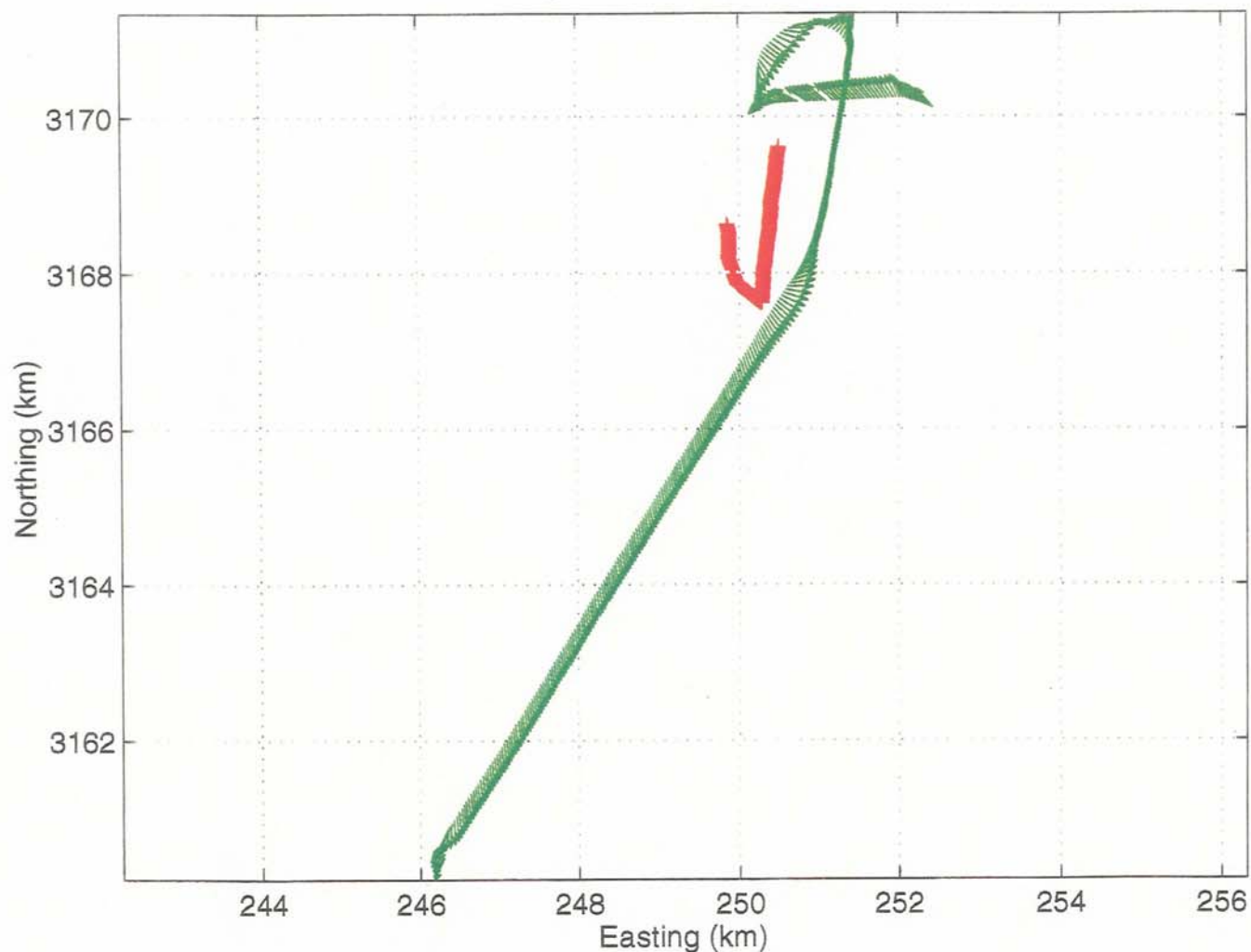


Figure 5. Experiment 4—Up-slope test geometry. The red crosses indicate the position of the receiving vessel M/V Sea Storm. The position of the source vessel M/V Sea Star is indicated by the origins of the green arrows. See Figure 2 for an explanation of the orientation of the green arrows.

then executed to read the time series, convert Volts to μPa and to plot the time series on the screen.

The data processing first corrected for the bandwidth reductions caused by the Ithaco 10 Hz high pass filter and the 3.2 kHz low pass filters built into the normal sensitivity hydrophones. The compensating filters to flatten the filter and hydrophone rolloffs were designed using knowledge of the Ithaco and hydrophone filters. Both were one pole filters and IIR digital filters which were intended to remove their effects were designed using the standard bi-linear transform approach¹. Since hydrodynamic noise was a problem during this experiment, it was necessary to apply a second high pass filter to remove non-acoustic energy in the frequency domain dominated by hydrodynamic noise while retaining energy at higher frequencies. For this purpose a linear phase, eighth order high-pass Butterworth filter was applied to the data with a rolloff frequency (-6 dB) at 5 Hz. Thus a 10 Hz to 20 kHz band was retained for the acoustic level measurements. The total composite frequency response of the compensated data is illustrated in Figure 6 by the red curve. The green curve shows the analog frequency response of data collection system itself.

The filtered data were then processed to measure the average pulse pressure. This was computed by summing the square of the pressure over the pulse duration, multiplying by the sample interval, dividing by the pulse duration and multiplying by two. The pulse duration was defined to be the interval between which 10 to 90% of the energy in the time series accumulated. The average pulse pressure is the acoustic exposure metric used in investigations of the effects of underwater noise on migrating gray whales in California (C.I. Malme, P.R. Miles, C.W. Clark, P. Tyack and J.E. Bird, "Investigations of the potential effects of underwater noise from petroleum industry activities on migrating gray whale behavior/ Phase II: January 1984 migration," BBN Report 5586, for US Minerals Manage. Serv, Anchorage, Al). "Malme et. al. expressed the average pulse pressure as the effective peak pressure of an equivalent constant-amplitude sine wave with the same pulse duration.

The corrected data were also measured for the peak amplitudes (positive or negative) of the direct blast and subsequent arrival structure associated with each source event. For

¹ A. V. Oppenheim and R. W. Schaffer, Digital Signal Processing (Englewood Cliffs, New Jersey: Prentis-Hall, 1975) 206-211.

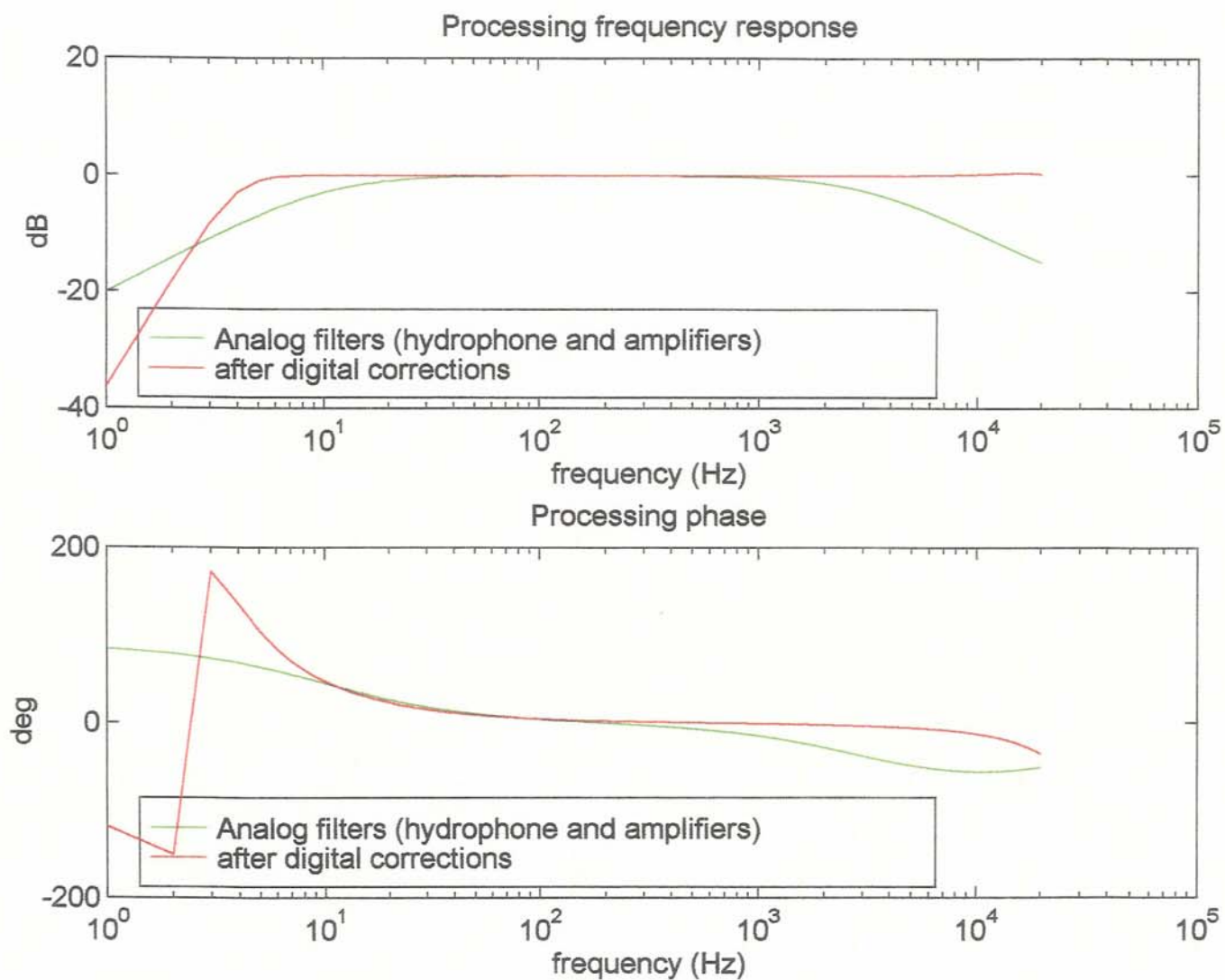


Figure 6. Low and highpass analog filters (green) and the corrective effect of the digital compensating filter (red)

processing intended to estimate the peak output level of the source as a function of aspect angle, it was also necessary to measure the amplitude of the direct arrival alone. Data which were contaminated by hydrodynamic noise were excluded from analysis throughout the project.

3. Results

3.1 Source Level Estimation—Experiment 1

This experiment was used to measure broadside peak source level by isolating the direct arrival at short range for a number of azimuths. When possible, all the phones were used, and the declination angles varied from 29.7 deg at 158 m to 4.28 deg at 1.2 km. These measurements were used as a check on the broadband peak source level of the array which had been estimated by Exxon using MODGUN prediction software².

Once the direct blast peak amplitudes from Experiment 1 were selected and measured, the navigation data was used with the time series data to estimate the source level. Initially a 20 log R spherical spreading correction was used to correct the peak direct blast levels to peak source levels at 1 m. However, when the derived source levels were plotted as a function of range, it was determined that the loss actually occurred at a higher law of approximately 25 log R. This result is related to the shallow source depth and its large horizontal extent, i.e. this law includes directive effects and the Lloyd mirror effect which can substantially reduce the direct blast peak amplitude at shallow angles relative to the surface.

The actual peak amplitudes received as a function of range at various depths for the close pass experiments are illustrated in Figure 7. Solid lines indicate peak levels from the direct blast, and + indicates peak levels which are measured at times later than the direct blast. Missing data, indicated by the gaps in the solid lines, indicates that the channel clipped or that the data was in some way corrupted.

From Figure 7, it is clear that the source passed to within approximately 158 meters of the vertical array. The peak direct blast level received was 197 dB re μ Pa at a range of 150m on the 80 m desensitized phone. At this range the 90 and 30 m phones clipped, indicating a pressure exceeding approximately 191.5 dB re μ Pa on those phones,

² MODGUN results provided by Mr. Raymond Young of Exxon Exploration Co., October 24, 1995

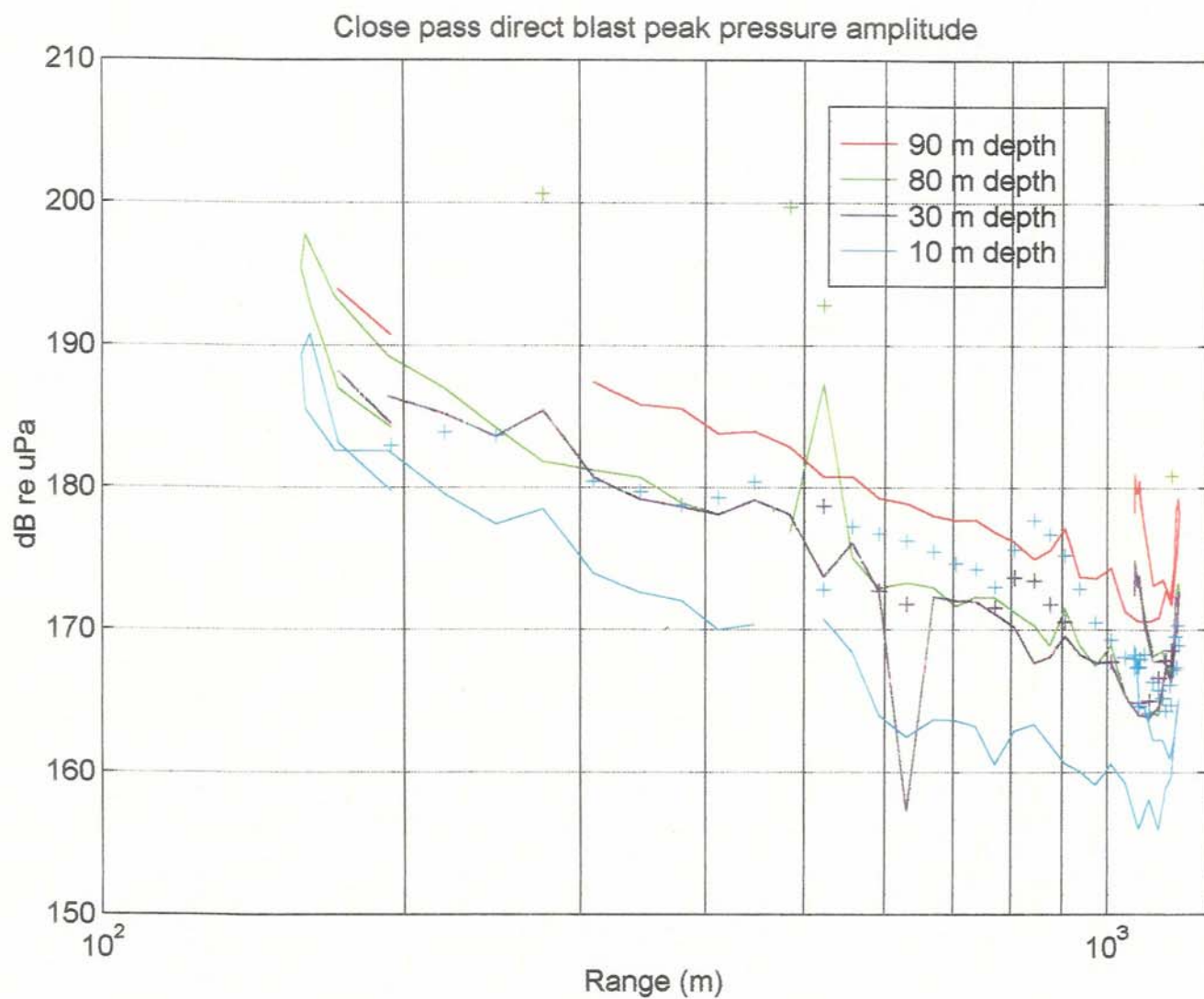


Figure 7. Peak amplitudes measured during the close pass experiment as a function of range.

although the 10 m phone, being already somewhat attenuated by the Lloyd mirror, recorded a peak pressure of 191 dB re μPa at this range. At slightly larger ranges still under 200 m, both the 30 and 90 m hydrophones were able to record levels unclipped. The 30 m phone agrees very closely with the 80 m desensitized phone at ranges between 171 and 193 meters, while both of these phones peak levels lie somewhat between the peak levels of the 90 m and the 10 m phone. Beyond 200 m, all direct blast amplitudes are lower than 190 dB re μPa , however the array angle has changed such that the receiver is no longer in the broadside direction.

Using the 25 log R propagation law, peak source levels as a function of range for various depths were derived: these are illustrated in Figure 8. It is clear that the source level estimated by the 25 log R propagation loss exceeds the estimate provided by Exxon, being approximately 255 dB re $\mu\text{Pa}\cdot\text{m}$ at broadside incidence on the 80 and 90 m phones rather than the 247 dB re $\mu\text{Pa}\cdot\text{m}$ discussed in Section 1. To interpret Figure 8 it is necessary to understand that the data collected at the closest and farthest ranges (158 m and 1.063 km) were both near broadside incidence, as referral to Figure 2 shows.

3.2 Broadside to endfire ratio

The broadside to endfire ratio was analyzed using both the close pass of experiment 1 and the long range data.

When analyzing the close pass data, the 25 log R propagation law was used to compensate for range. Inadequately compensating the source levels as a function of range would result in an over-estimate of the broadside to side-lobe ratio. Using the 25 log R propagation law, the source peak level directivity function illustrated in Figure 9 is obtained. This directivity function was parameterized by the linear curve superimposed on the figure, which has a peak amplitude of 8.5 dB in the 90 deg direction and 0 deg in the end-fire direction. 8.5 dB broadside to end-fire ratio compares favorably with MODGUN model results which gave 8.5 dB for a 10 deg D/E angle. This linear parameterization with the 8.5 dB ratio was used to compensate for directivity for all other propagation measurements.

The figure-eight patterns conducted during long range propagation experiments were also designed to obtain in-situ broadside to end-fire source level ratios averaged over all D/E angles. The broadside to end-fire ratios measured for the 5 km figure-eight in Experiment 4 were found to be highly variable. Since the broadside to end-fire ratios

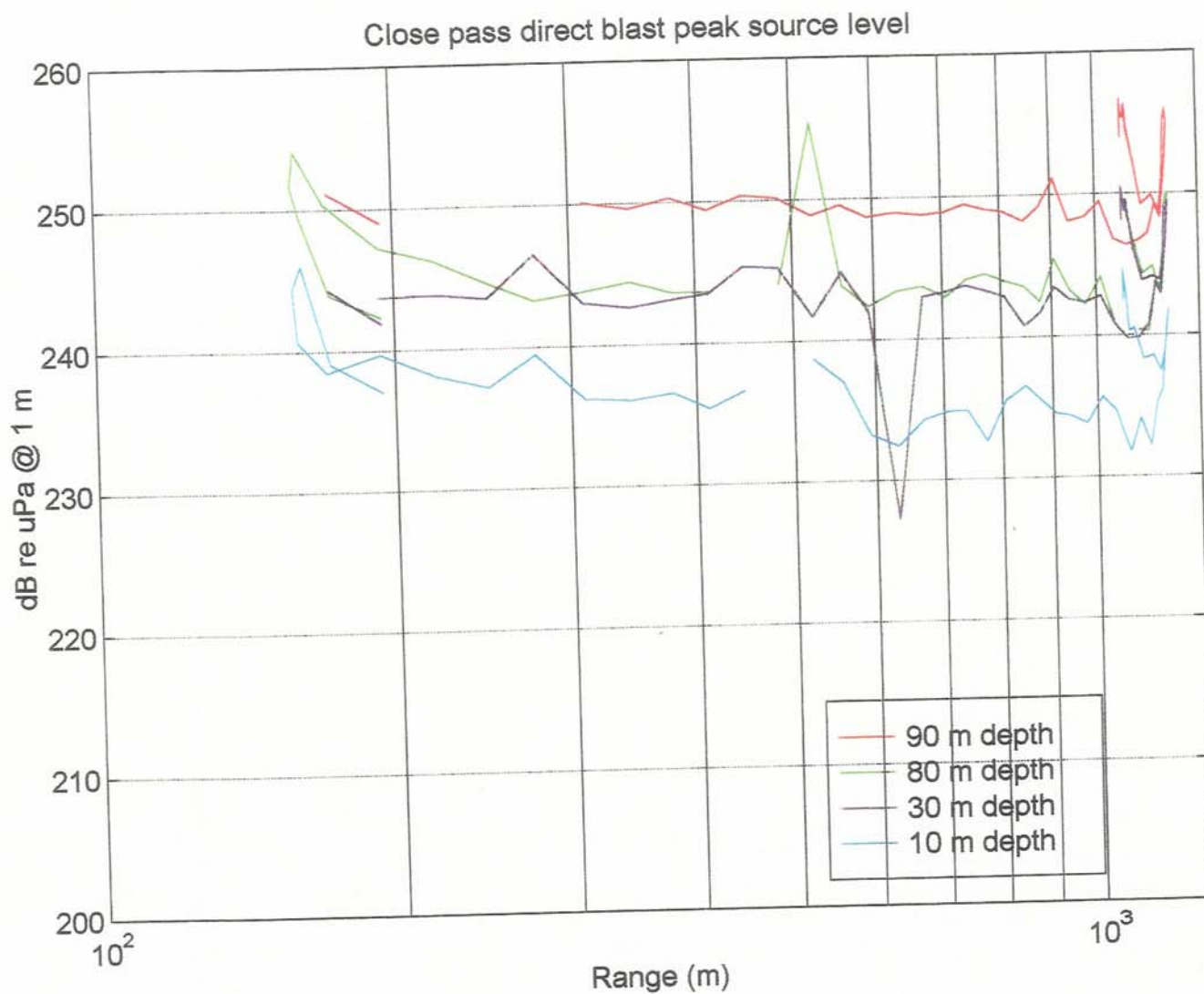


Figure 8. Peak source levels estimated from close pass peak amplitudes, as a function of range

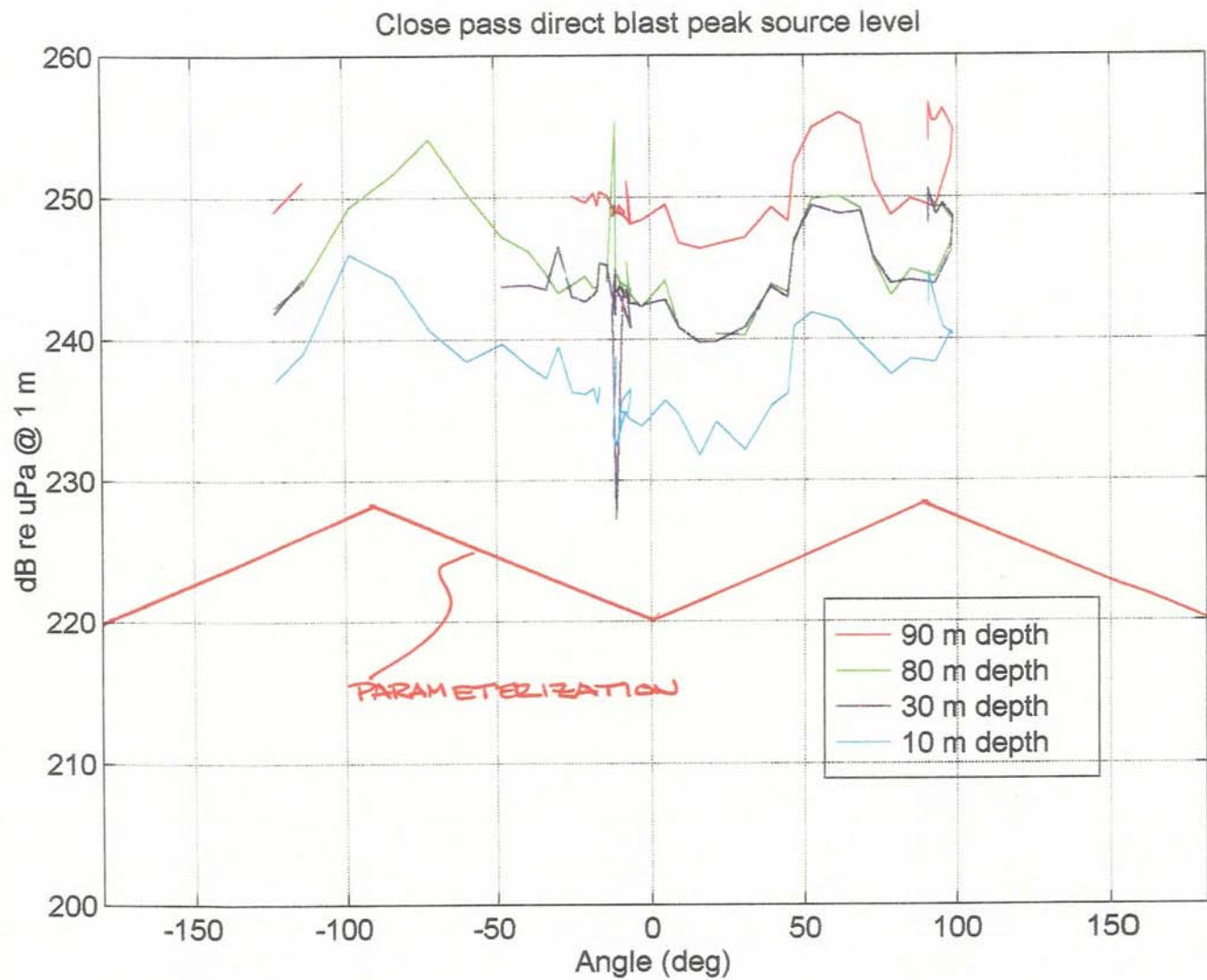


Figure 9. Peak source levels as a function of array to receiver bearing.

observed on the 5 km figure-eight were less than or equal to the ratios observed in the close pass experiment, the more conservative 8.5 dB correction was used for the long range propagation data.

3.3 Determination of $X \log(\text{range})$ propagation law and isopleths

The different experiments were designed to estimate the acoustic levels as a function of range under different propagation conditions. Experiment 1 provided close range measurements for determining the ranges for the 190 and 180 dB re μPa isopleth. Since it is known that bathymetry strongly effects propagation, Experiments 2, 3, and 4 were laid out to measure long range propagation in the down-slope, cross-slope and up-slope directions respectively.

The average pulse pressures were corrected for the array to receiver aspect angle and plotted as a function of range. Super-imposed on the data points are best fit estimates of a simple $X \log R$ propagation law, which can be assumed to capture the essentials of the propagation in the near field. Data from all hydrophone depths were used in these fits to get a representation of the average levels expected at a range. In order to exclude anomalous values a least absolute value (L1) norm fit was used rather than least squares. A second line is drawn on the figures which represents a 90% confidence line, below which 90% of the measured levels fall. The L1 fit is a least absolute value norm, which returns a fit where half of the data lie above the regression curve and the other half lie below it. The fit was performed in the dB domain, as it is generally recognized that sensitivity to sound is best related to logarithmic measures. Obtained in this way, the L1 regression provides a curve below which 50% of the average pulse pressures can be expected at any given range. In order to quantify the spread in the distribution of the average pulse pressure levels, a "90% confidence limit" curve below which 90% of the observations lie was also obtained. This curve always lies above the L1 regression, which is equivalent to the 50% confidence limit. In our approach, the statistics of the average pulse pressure distribution about the 50% confidence line are assumed to be uniform in range, resulting in a 90% confidence limit which is parallel to the 50% confidence limit.

Because of the way the whale avoidance statistics were calculated in the original studies by Malme et. al., the L1 regression, 50% curve which parameterizes the average exposure at a given range, is the proper measure with which to calculate the isopleths to the 190,

180 and 160 dB re μPa average pulse pressure levels. The 90% confidence intervals are reported in the interest of quantifying the spread of the observed average pulse pressure distributions, but are not appropriate for determination of isopleths as they are not consistent with the statistical methodology used by Malme et. al. to determine that 160 dB re μPa average pulse pressure caused 10% avoidance by gray whales.

3.3.1 190 dB re μPa isopleth

The short range measurements of Experiment 1 were used to determine the range to the 190 dB re μPa average pulse pressure isopleth. For this data, the analysis interval usually included the direct arrival, unless the hydrophone was very shallow. For the shallow hydrophone, the Lloyd mirror effects reduced the observed level of this portion of the signal and the bottom bounce was dominant. The analysis integration window always included some portion of the arrival structure consisting mostly of bottom multiples, except for the deepest hydrophones at very short range, when the direct blast often carried more than 90 percent of the total energy of the waveform. The average pulse pressures were corrected for broadside to end-fire ratios using the linear beam-pattern parameterization discussed above and were used to estimate the maximum distances at which average pulse pressures exceed 190 dB.

It can be observed that the direct blast average pulse pressure levels died out quickly in the vicinity of the closest point of approach (CPA). This was due in part to directivity effects in the vertical plane. Inspection of Figure 10 reveals that the average pulse pressure at a range of 200 m is approximately 183 dB re μPa , depending on depth. As range is increased, the best model fit to the average pulse pressure amplitude is $29.9 \log R$ with an average pulse pressure source level of 251.3 dB re μPa . This parameterization yields average pulse pressures above 190 dB re μPa out to ranges of 110 meters.

3.3.2 Determination of the 180 dB re μPa isopleths

For Experiment 1, the range to the 180 dB re μPa average pulse pressure isopleth for the measured data increases with receiver depth. As with the 190 dB isopleth this result is due to the extended nature of the source combined with Lloyd's mirror effects. Using the line fit over all the hydrophones, the corrected range to the 180 dB re μPa average pulse pressure isopleth is 244 m. These results were obtained in 500 m of water, and should be expected to vary considerably with water depth. This is because the estimated pulse duration which affects the average pulse pressure measure was often found to include

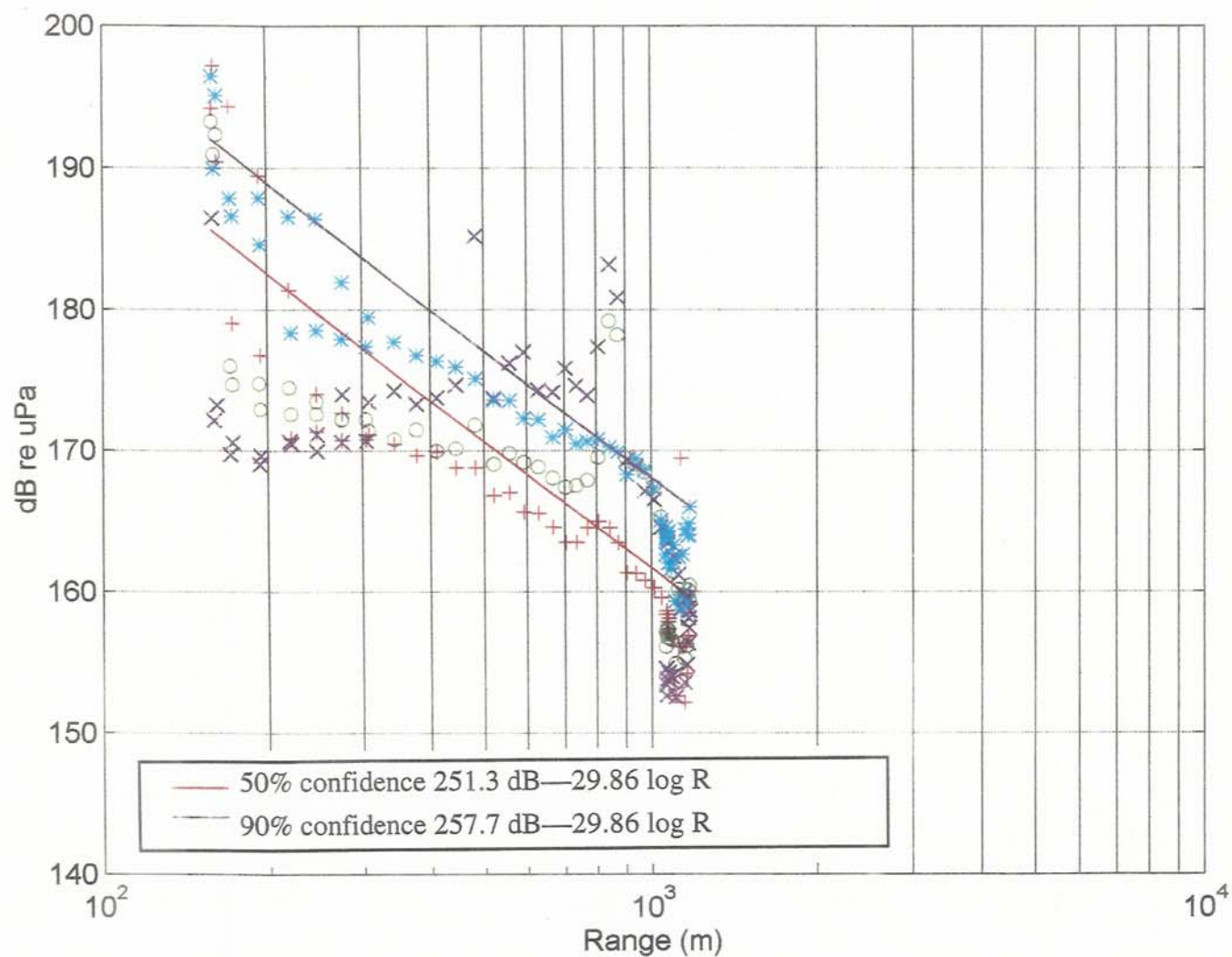


Figure 10. Experiment 1—Average pulse pressure level as a function of range (endfire corrected +8.5 dB)

both the direct blast and the bottom bounce. Shallower water would have the effect of reducing the time interval required to exceed 90 % of the pulse energy, thus increasing the average pulse pressure metric.

3.3.3 Determination of 160 dB re μ Pa isopleth for Experiments 2, 3 and 4

For the long range experiments, the integration window used to compute average pulse pressure level would typically include about 90 percent of the observable arrival structure. No particular arrival would contribute a predominant portion of the energy. The average pulse pressure as a function of range for Experiment 2 is illustrated in Figure 11. During this experiment, the acoustic propagation was down-slope. The average pulse pressure has several local maxima, at ranges of 3.6, 6, 8 and 9 km. These maxima are caused by propagation effects in downward refracting media, and are the first, second, third and fourth bottom multiples. The low levels between the peaks represent shadow zones of propagation. If the nearfield shadow zone results at ranges less than 3 km are excluded from the fit, then the propagation law as fit to all the hydrophones is a $288.7 - 33.18 \log R$. This gives a range to the 160 dB re μ Pa isopleth of 7566 m for down-slope propagation. For this experiment which starts at 1 km, effectively all average pulse pressure levels were below 180 dB, as a result of the first shadow zone.

For Experiment 3, the cross-slope experiment, the bottom multiple propagation characteristics as seen in Experiment 2 are also present. The cross-slope average pulse pressure as a function of range measured during Experiment 3 is plotted in Figure 12. Bottom multiples are clearly evident at ranges of 3, 5 and 7 km, similar to the down-slope results. The propagation loss is a stronger function of range, indicating that bottom losses are greater in the constant depth scenario. As the grazing angles are greater in up and cross-slope geometries than in down-slope, and as interaction losses increase with increasing grazing angles, the higher power law range dependence for this experiment is expected. When the first shadow zone is excluded from the L1 fit, the average pulse pressure obeys a $273.9 - 29.8 \log R$ propagation law, which results in a range to the 160 dB re μ Pa isopleth of 6640 m.

As opposed to the cross and down-slope experiments, the up-slope propagation of Experiment 4 shows little evidence of bottom multiple propagation, and also displayed much higher losses as a function of range. Inspection of Figure 13 shows that, with the possible exception of a shadow zone at ranges of less than 1 km and a convergence zone

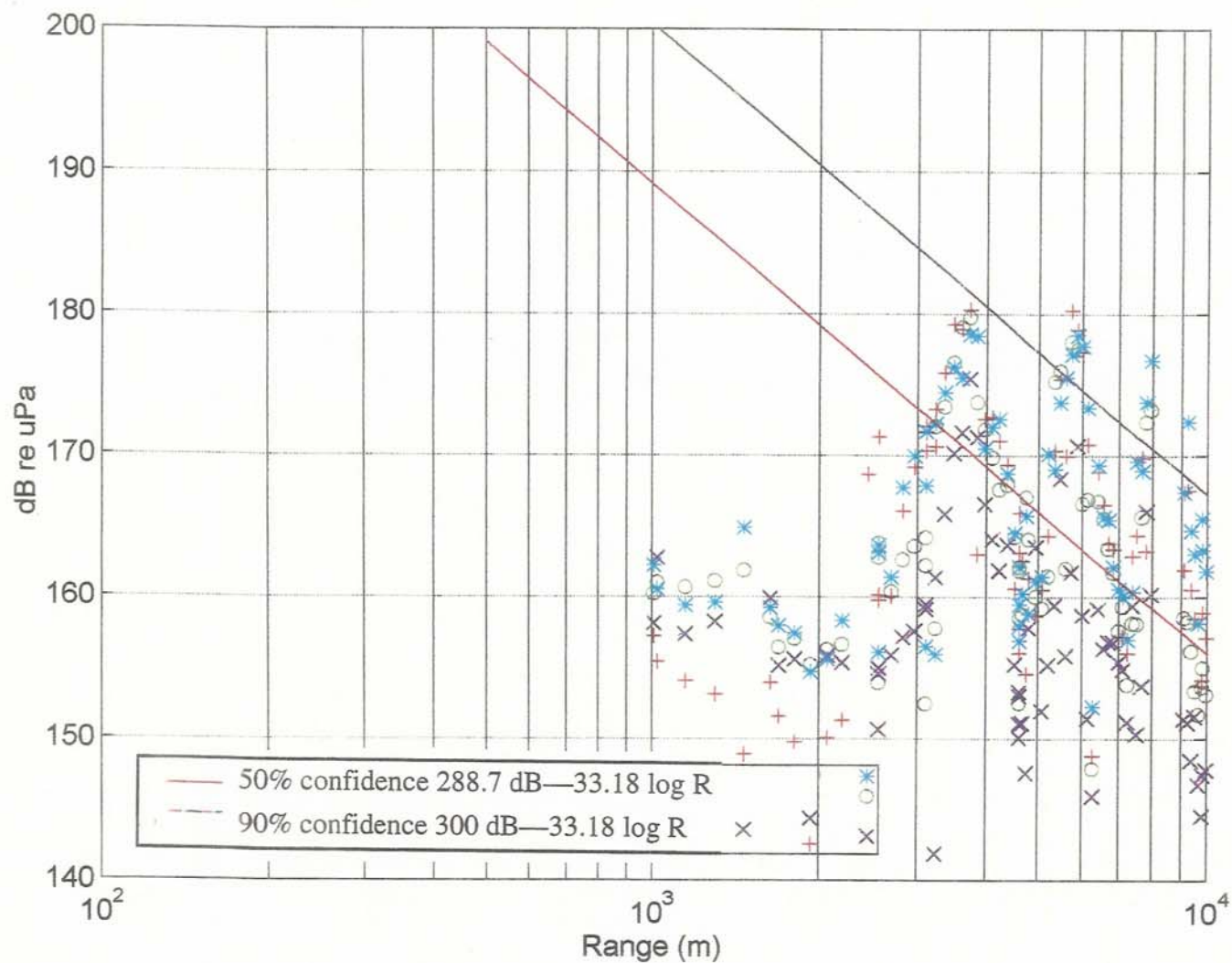


Figure 11. Experiment 2—Average pulse pressure level as a function of range (endfire corrected +8.5 dB)

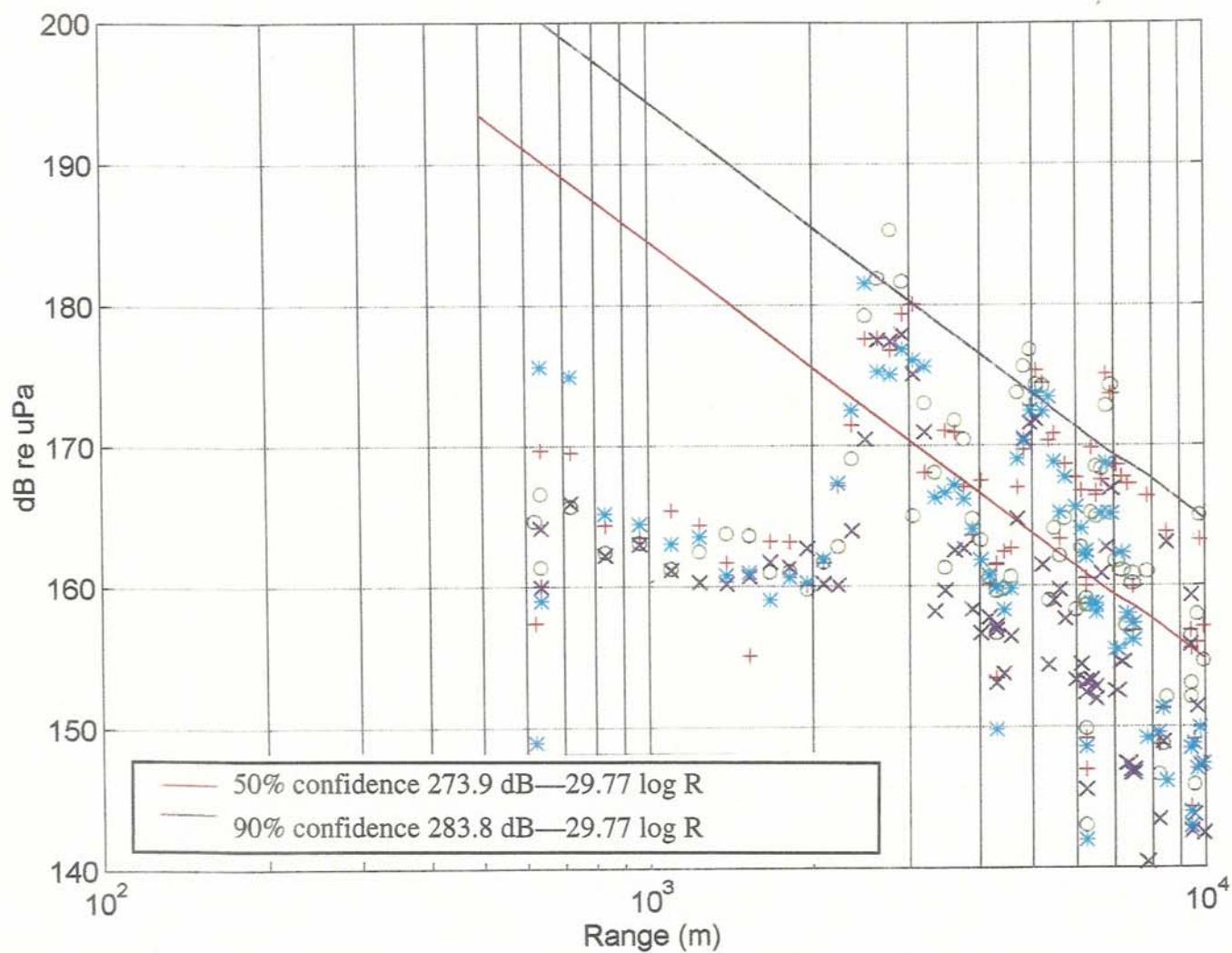


Figure 12. Experiment 3—Average pulse pressure level as a function of range (endfire corrected +8.5 dB)

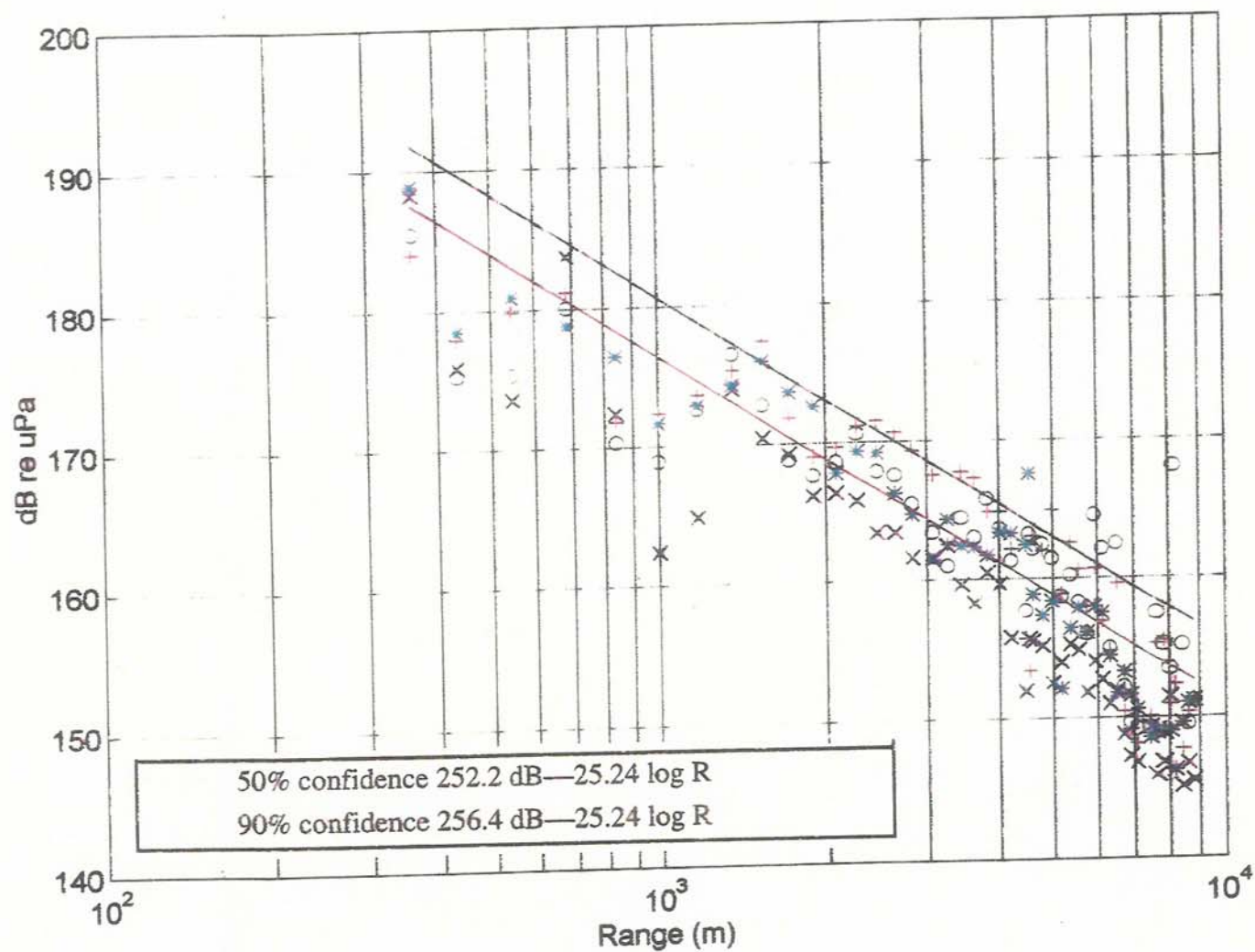


Figure 13. Experiment 4—Average pulse pressure level as a function of range
(endfire corrected +8.5 dB)

at 1.5 km, the average pulse pressure falls monotonically with increasing range, yielding a $252.2 - 25.24 \log R$ propagation law when parameterized with a L1 fit between the ranges of 500 meters and 10 km. This law yields a distance of 4497 meters for an average pulse pressure of 160 dB re μPa .

4. Conclusions

The results of the close pass analysis confirm the expected source characteristics of the airgun array. Through observation of the direct blast, we found that the source level of the airgun array was approximately 255 dB re $\mu\text{Pa}\cdot\text{m}$, corresponding to a source level of 56.2 bar-m. This source level exceeds the estimated source level of 247 dB re $\mu\text{Pa}\cdot\text{m}$ at broadside by 8 dB, which is within the tolerance of the experiment. We also observed peak broadside to sidelobe ratios of approximately 8-10 dB, results which are in close agreement with the 8.5 dB peak to sidelobe ratios predicted by the MODGUN model employed by EXXON. Based on these results, we conclude that the source utilized in this study has been well characterized by the experimental observations, and that the results are in good agreement with those predicted by theory.

From the close pass Experiment 1, we were able to predict isopleths for 190 and 180 dB re μPa average pulse pressures of 110 and 244 meters, these results were obtained in 500 m of water, and should be expected to vary considerably with water depth. These results are summarized in the first two rows of Table 4.

Table 4. Ranges to the 190, 180 and 160 dB re μPa average pulse pressure isopleths for the Mississippi Canyon experiment. The three ranges given for the 160 dB re μPa isopleth are for three different propagation scenarios of down, cross and up-slope

Average Pulse Pressure	Range	Scenario			
dB re μPa	Meters	Close-Pass	Down-Slope	Cross-Slope	Up-Slope
190	110	✓			
180	244	✓			
160	7566		✓		
	6640			✓	
	4497				✓

Three 160 dB re μ Pa isopleths were determined from average pulse pressure analysis of the three long range experiments. Ranges of ^{7.6}10, 6.7 and 4.5 km were obtained for the down-slope, cross-slope and up-slope propagation scenarios, respectively. These results indicate an increasing harshness of propagation conditions with the increasing angles of bottom incidence commensurate with propagation in shoaling geometries. These results are entirely consistent with the known propagation characteristics of acoustic energy in shallow water, downward refracting waveguides. These results are summarized in the last three rows of Table 4.